

# Determination of Power Line Transfer Functions by a Method of Impedance Transfer and Voltage Spread

Thanakorn Khongdeach<sup>\*</sup>, Wachira Chongburee, and Nattaka Homsup

**Abstract**—A novel method to determine the transfer functions of power line networks is presented. Although a number of the evaluation methods have been proposed, the major drawbacks are on approximation, complexity and intuitiveness. The presented method overcomes those by making use of backward impedance transfer and forward voltage transfer techniques. Additionally, the method offers an extra feature that transfer functions at any points throughout the network can be determined in one implementation. This paper first reviews some major existing methods. Then, the method of impedance and voltage transferring is derived and fulfilled with an implementation algorithm and mathematic description. Lastly, an implementation of the method on a sample network for the transfer function is demonstrated. Channel capacity is adopted as the measure for the quality of the channels.

## 1. INTRODUCTION

There are several choices of communication media with various advantages and disadvantages available for certain applications and scenarios. When choosing the media, cost definitely comes into the consideration. To preserve the cost, the existing power lines can be used as a communication media without an investment on the infrastructure. However, it is always a tradeoff between cost and performance. The power line network is optimized for power delivery purposes. Its performance as a communication media is limited.

The characteristics of the components in the power line network are an obstacle for being a good communication media. For example, impedance mismatches, which cause signal reflection, are commonly found throughout the power line network. As a result, the power line cannot be considered as a good communication media. Moreover, branchy power line networks are prone to exhibit signal reflection. The communication on such a networks gets worsen, generally. Therefore, the knowledge of network frequency responses is one of valuable measures of the power line performance as a communication media.

The organization of this paper is as the follows. The existing methods to determine the frequency responses of the power line network are briefly reviewed in the next section. In Section 3, the basic ideal of the proposed method is discussed. An implementation procedure is also provided. Section 4 compares the results from using the proposed method and from a commercial software. Section 5 presents a method to describe the networks in a matrix form along with a closed form of the transfer functions. An implementation of the proposed method on a sample network to obtain the transfer functions at any destinations in the network is demonstrated. Finally, the conclusion is drawn in Section 6.

## 2. EXISTING METHODS

The existing methods used to determine the frequency response of power line communications might be categorized into two approaches. The first approach is to trace the signal paths. This approach can be

---

*Received 2 April 2018, Accepted 24 June 2018, Scheduled 26 July 2018*

<sup>\*</sup> Corresponding author: Thanakorn Khongdeach (g5317500320@ku.ac.th).

The authors are with the Department of Electrical Engineering, Kasetsart University, Bangkok, Thailand.

implemented either in the time domain or in the frequency domain, while the other approach models the power line network by a cascade of functional blocks. This approach does not require signal path tracing.

## 2.1. Signal Path Tracing Approach

In this approach, the power line network is driven by an impulse. Every time the impulse travels on a power line and reaches a mismatched impedance joint, it generates two impulses. One goes through the joint, and the other reflects back. The magnitudes of the through and the reflected impulses can be determined from a reflection coefficient, which is calculated from the two mismatched impedances at the joint. The resulting received impulse response  $h(t)$  at one specific destination is the sum of the infinite number of the delayed impulses from all reflecting paths. Assuming  $N$  paths are dominating, an approximation of the impulse response is given by [1]

$$h'(t) = \sum_{i=1}^N g_i A(f, d_i) \delta(t - \tau_i) \quad (1)$$

where  $g_i A(f, d_i)$  is the resulting magnitude of the impulse of path  $i$  with a delay of  $\tau$ . It can be obtained by the multiplication all of the reflection coefficients, the transmission coefficients and the total ohmic loss of the  $i$ th path. The desired approximated version of transfer function  $H'(f)$  is simply the Fourier transform of  $h'(t)$ . For a simple network as in Fig. 1, some paths from the source to Destination 1 are  $A \rightarrow B \rightarrow D$ ,  $A \rightarrow B \rightarrow C \rightarrow B \rightarrow D$ ,  $A \rightarrow B \rightarrow A \rightarrow B \rightarrow D$  and there are still many more paths. It is not obvious to tell which paths are dominating. As a consequence, the difficult part of this approach is on the tracing for the dominating paths.

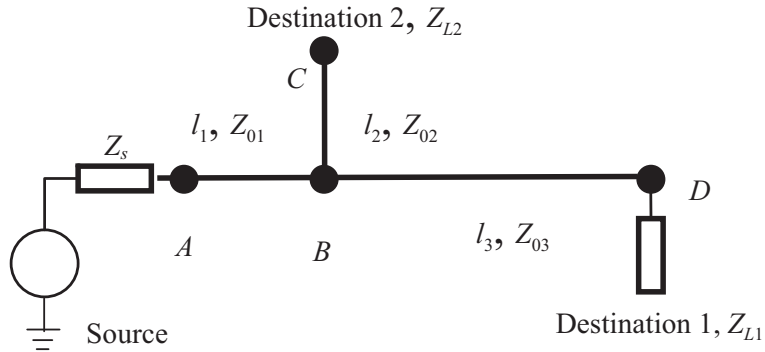


**Figure 1.** A simple network.

Another method in this class is found in [2, 3]. This method traces the signal traveling paths as well but the tracing is implemented directly in the frequency domain. According to the method, a frequency-dependent incident voltage  $v_+$  travels from the voltage source to the power line network. When it reaches an interconnection of impedance-mismatched lines, the voltage partially reflects back and partially transmits to the connected branches. The reflected voltage behaves as a newly generated voltage source. A new voltage source keeps being induced every time the voltage hits a mismatched interconnection. As a result, the number of induced sources goes to infinity. Nevertheless, the magnitude of the newly generated source, on the other hand, decreases. The transfer function  $H(f)$  is then computed from the ratio of the sum of the voltages that eventually come to the sink of interest  $V_L(f)$ , and the incident voltage  $v_+$ .

The complexity of this approach is about the same as the previous time domain approach since it requires a similar path tracing. Hence the complexity exponentially increases when an extra branch or interconnection is added to the network. The final result is only an approximated version of the transfer function due to the finite number of paths invoked by the approach. Another major inflexibility is that the transfer function is particularly for one destination. If a transfer function at another place on the

power line network is needed, the signal reflection paths have to be completely rerouted. The next method is less demanding on this issue.

### 2.2. Cascade Block Approach

The other class of existing techniques to find the transfer function parses the network into blocks. A technique by [4] models the power line network by an *overall*  $2 \times 2$  matrix called *ABCD* matrix. The left end of this matrix is connected to a source voltage  $V_s$  with a source impedance  $Z_s$  while the right end is connected to the load  $Z_L$ . The input-output relationship of the voltages and currents is given by

$$\begin{bmatrix} V_{in} \\ I_{in} \end{bmatrix} = \begin{bmatrix} A & B \\ C & D \end{bmatrix} \begin{bmatrix} V_L \\ I_L \end{bmatrix} \tag{2}$$

The transfer function defined by  $V_L/V_s$  can be determined from the matrix elements by

$$H(f) = \frac{V_L}{V_S} = \frac{Z_L}{AZ_L + B + CZ_SZ_L + DZ_S} \tag{3}$$

The overall matrix is decomposed into sub-matrices in a cascade configuration as illustrated in Fig. 2. For instance, the sub-matrix for a power line is given by

$$\begin{bmatrix} A_1 & B_1 \\ C_1 & D_1 \end{bmatrix} = \begin{bmatrix} \cosh(\gamma_1 l_1) & Z_{01} \sinh(\gamma_1 l_1) \\ \frac{\sinh(\gamma_1 l_1)}{Z_{01}} & \cosh(\gamma_1 l_1) \end{bmatrix} \tag{4}$$

where  $\gamma_1$  and  $l_1$  are the line propagation constant and power line length, respectively. On the other hand, if the sub-matrix represents a branching line with an terminating impedance  $Z_{L2}$ , the sub-matrix becomes

$$\begin{bmatrix} A_2 & B_2 \\ C_2 & D_2 \end{bmatrix} = \begin{bmatrix} 1 & 0 \\ \frac{C_b Z_{L2} + D_b}{A_b Z_{L2} + B_b} & 1 \end{bmatrix} \tag{5}$$

where  $A_b, B_b, C_b$  and  $D_b$  are the elements of the branching line matrix. The multiplication of them yields the overall matrix which is used to determine the transfer function as discussed earlier.

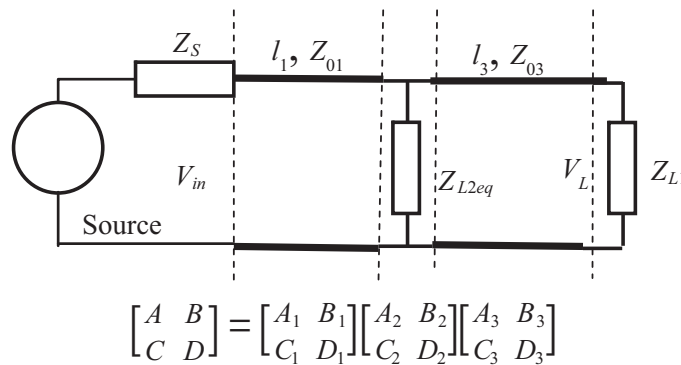


**Figure 2.** *ABCD* matrix models.

In addition to the *ABCD* method, a cascade approach to determine the transfer function is discussed in [5–7]. The approach models the printed circuit board (PCB) networks by a tree of *L*-cells. Each cell represents a piece of transmission line strip on a PCB. The cell is formed by a series impedance and a parallel admittance, which can be represented by a  $2 \times 2$  transfer matrix *T*. The entire network is viewed as a tree topology so it is a form of a single input multiple output (SIMO) network. Each branch of the tree can be modeled by an *L*-cell as well. Combining the *L*-cells turns the SIMO network into a cascade single input single output (SISO) network. This SISO can be described by an overall transfer  $2 \times 2$  matrix. The voltage transfer function is simply the reciprocal of the first entry for the overall matrix.

Another approach in this class [8] invokes a model of impulse invariant response (IIR) filters. The idea behind this approach is that the signals on the power line network undergo infinite bounces, which are like the responses of IIR filters. In this approach, parts in the power line networks are categorized into modules such as lossless line, T-junction, star junction, serial and parallel impedances. Each module is then described by a set of four transfer functions,  $H_f$ ,  $H_b$ ,  $\tilde{H}_f$  and  $\tilde{H}_b$ . These are derived from four possible combinations of two ports and two entering/leaving directions of the signals. When two modules are connected, the transfer functions are updated uniquely for each type of the modules. Hence, the complexity rises exponentially when an additional module is added to the chain.

These methods are not quite flexible when it comes to determination of the multiple transfer functions on the power line network. This is because the methods in this class require a chain of blocks linking the source to a particular destination. Therefore, a new set of blocks must be created for each particular destination in the power line network.

A remarkable method proposed in [9] aims to determine the frequency responses at multiple destinations. The concept is that the complex network is divided into a number of single-junction units. The key is on the update of the reflection coefficients. The method is powerful albeit rather additively complicated. It is possible to implement a similar approach which is also based on the same transmission line theory but simplicity and intuitiveness are relatively improved. An alternative method called shrink and spread, which is simpler and more straightforward, is discussed in the next section.

### 3. SHRINK AND SPREAD METHOD

Recently, a method to find the transfer function named Backward Impedance Transfer (BIT) [10] that overcomes the disadvantage of being particular on the destination was introduced. The method delivers an exact version of the transfer function not just an approximated version. It is relatively simple, yet computation friendly and dramatically intuitive. Essentially, it allows determination of multiple transfer functions at any places on the power line network without re-routing for specific signal destinations. This section discusses details and develops the method further to complete its usability.

#### 3.1. The Basic Idea

The idea of BIT is that the entire power network is folded down or shrunk into a single impedance connected right to the source called  $Z_{in}$ . According to a basic microwave theory, a branch of length  $l$  with a terminating load  $Z_L$  can be collapsed into a *transfer* impedance  $Z'$  by the relationship

$$Z' = \mathbf{T}\{Z_L, l\} = Z_0 \left[ \frac{Z_L + Z_0 \tanh(\gamma l)}{Z_0 + Z_L \tanh(\gamma l)} \right] \quad (6)$$

where  $\gamma$  and  $Z$  are the propagation constant and characteristic impedance of the transmission line, respectively. Note that in this paper, the operator  $\mathbf{T}\{\cdot\}$  denotes a transfer operation of a terminating impedance  $Z_L$  over a power line of length  $l$  to a transfer impedance  $Z'$ . To achieve  $Z_{in}$ , the furthest branch from the source is to collapse first. The folding down process is kept going towards the source. When multiple branches are met at an interconnection, the transfer impedances of branches are combined parallel. Eventually, the entire network will be replaced by one impedance called  $Z_{in}$ .

Next, the initial voltage  $V_{in}$  across  $Z_{in}$  is to be calculated by the voltage divider

$$V_{in} = V_s \frac{Z_{in}}{Z_{in} + Z_s} \quad (7)$$

where  $Z_s$  is the internal source impedance. Once  $V_{in}$  on one end of a power line is known, the voltage  $V_L$  on the impedance  $Z_L$  across a power line of length of  $l$  and a characteristic impedance of  $Z_o$  is given by

$$V_L = V_{in} \left( \frac{1 + \Gamma_L}{e^{\gamma l} + \Gamma_L e^{-\gamma l}} \right) = V_{in} \cdot \mathbf{F}\{\Gamma_L, l\} \quad (8)$$

where  $\gamma$  is the propagation of the transmission line and  $\Gamma_L$  is the reflection coefficient defined by

$$\Gamma_L = \frac{Z_L - Z_0}{Z_L + Z_0} \quad (9)$$

The operator  $\mathbf{F}\{\cdot\}$  can be viewed as a voltage gain that forwards  $V_{in}$  along the power line to the load  $Z_L$ . The voltages are kept forwarded until reaching the terminating impedances in a spreading out fashion. Eventually, the voltages all over the network are established and so are the associated transfer functions. Note that a transfer function is just the ratio of the voltage on a designated load  $V_L$  and the source voltage  $V_s$ .

The next section generalizes this shrink-spread method for a network of  $N$  nodes with up to  $B$  branches connected to each node. An algorithm to compute the transfer functions is discussed, and the mathematic expressions for the shrinking and spreading processes are derived.

### 3.2. Physical Network Description

At a first glance, the network topology is assumed non-nested. It means that the voltage source is connected to one main line, and the branches can only be tapped off from one of the interconnections on the main line. They will be terminated by an impedance. There are no additional interconnections on the branches. Nested networks will be discussed later. The network topology is depicted in Fig. 3.

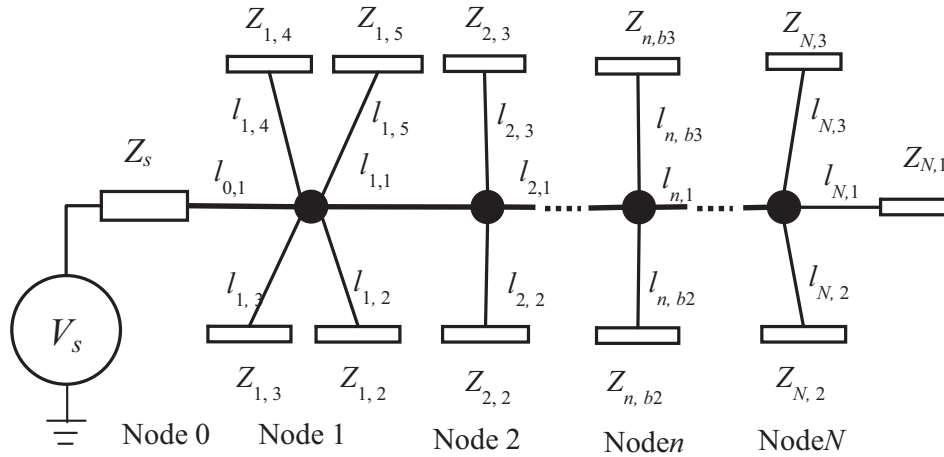


**Figure 3.** Network topology with terminating impedances at the end of the branches.

The network parameters can be described by a set of matrices conformed to the network topology as the follows. Starting from the source side, the first interconnection between the source impedance and the line is defined by Node 0. The interconnection toward the right are numbered by Node 1, Node 2 and so on until the last Node  $N$ . At Node  $n$ , there will be one main line running rightward to the next node, Node  $(n + 1)$ . It is referred to by  $Line(n, 1)$  where  $n$  represents the node number and 1 implies that it is the main line. Other regular branching lines that are tapped off from Node  $n$  are named  $Line(n, b)$  where  $b = \{2, 3, \dots, B_n\}$ , and each is terminated by an impedance  $Z_{n,b}$ .

Hence, the network topology can be described by an  $N \times B$  matrix of length,

$$L_{Length} = \begin{bmatrix} l_{1,1} & l_{2,1} & \dots & l_{N,1} \\ l_{1,2} & l_{2,2} & \dots & l_{N,2} \\ \vdots & \vdots & \ddots & \vdots \\ l_{1,B} & l_{2,B} & \dots & l_{N,B} \end{bmatrix} \quad (10)$$

where element  $l_{n,b}$  represents the length of  $Line(n, b)$ , the  $b$ th branch tapped off from the  $n$ th Node. The numbers of columns  $N$  and of rows  $B$  are equal to the total number of the interconnections (or the nodes) and the largest number of branches connected to the nodes, respectively. As assigned earlier, the 1st branch of Node  $n$  is always assigned to the main power line which draws from Node  $n$  to Node  $(n + 1)$  on its right. At the last Node  $N$ , branch number 1 can be assigned to any branches since no further nodes are on the right. It is noted that the matrix excludes the main line running from the source at Node 0 to the entrance of the network at Node 1. The line is denoted exclusively by  $Line(0, 1)$

with a length of  $l_{0,1}$ . When there are only  $B_n < B$  branches connected to Node  $n$ , the elements  $l_{n,b}$  in Eq. (10) for  $b > B_n$  are simply filled with 0.

The other necessary matrices to completely describe the line properties are (i) line capacitance per unit length  $C_{PU}$ , (ii) line inductance per unit length  $L_{PU}$ , (iii) line resistance per unit length  $R_{PU}$ , and (iv) line conductance per unit length  $G_{PU}$ . They can be indexed similarly to the ones used in the length matrix  $L_{Length}$ . These four matrices are used to derive the line characteristic impedance matrix,  $Z_{0,NB}$ . For a lossless network, matrices  $R_{PU}$  and  $G_{PU}$  can be neglected. It is noted that the characteristic impedance  $Z_{0,0,1}$  of  $l_{0,1}$  is not a part of these matrices.

Lastly, the network description is completed by a branch terminating impedance matrix,  $Z_{NB}$ .

$$Z_{NB} = \begin{bmatrix} TBD & TBD & \dots & Z_{N,1} \\ Z_{1,2} & Z_{2,2} & \dots & Z_{N,2} \\ \vdots & \vdots & \ddots & \vdots \\ Z_{1,B} & Z_{2,B} & \dots & Z_{N,B} \end{bmatrix} \quad (11)$$

The indexing is the same as that previously assigned. Again, when the number of branches  $B_n$  is less than  $B$ , the extra elements of matrix  $Z_{n,b}$ , where  $b > B_n$ , are simply filled by  $\infty$ . It is noted that the terminating impedances corresponding to the main line  $Z_{n,1}$  except  $Z_{N,1}$  are not yet known from the physical components of the network. They will be determined backwardly as detailed in the next section. Since the entries on the first row of the matrix in Eq. (11) except  $Z_{N,1}$  are not yet known, they can be initialized by any values, for example, TBD (to be determined).

### 3.3. Implementation of Line Shrinking

According to BIT method, the goal of the shrinking procedure is to obtain an impedance that represents the entire network. As illustrated in Fig. 4, the process starts by shrinking all branches to the main. It means that the terminating impedances  $Z_{n,b}$  are to be transferred over the line  $Line(n,b)$  to Node  $n$  and become  $Z'_{n,b}$

$$Z'_{n,b} = \mathbf{T}\{Z_{n,b}, l_{n,b}\} = Z_{0,n,b} \left[ \frac{Z_{n,b} + Z_{0,n,b} \tanh(\gamma l)_{n,b}}{Z_{0,n,b} + Z_{n,b} \tanh(\gamma l)_{n,b}} \right] \quad (12)$$

where  $Z_{0,n,b}$  and  $Z_{n,b}$  are the branching line characteristic impedance and the terminating impedance of  $Line(n,b)$ , respectively. The impedance transfer process is denoted by an operator  $\mathbf{T}\{\cdot\}$ . The parameter  $\gamma$  in Eq. (12) is the propagation constant of the line  $Line(n,b)$ . The resulting transferred impedances  $Z'_{n,b}$  will be kept in another  $B \times N$  matrix named  $Z'_{NB}$ . When all branches are transferred to  $Z'_{n,b}$ , a total number of  $B_n$  impedances are present at Node  $n$ .

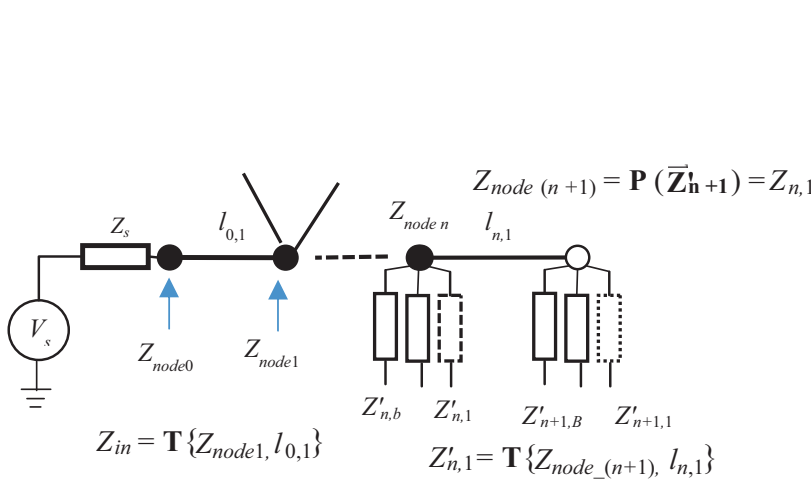


Figure 4. The flow of network shrinking.

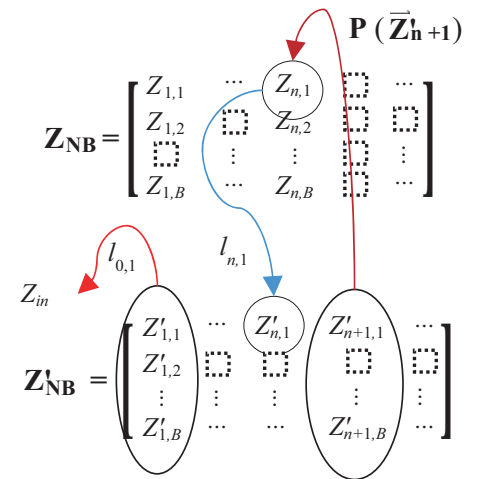


Figure 5. Updating the matrices.

The entries on the first row of matrix  $Z'_{NB}$  which are  $Z'_{n,1}$  for  $n = 1$  to  $N - 1$  cannot be calculated promptly. Calculation for the entries  $Z'_{n,1}$  requires a special treat since the line  $Line(n, 1)$  is on the main and is connected to the next node,  $(n + 1)$  rather than an explicit physical impedance. To find  $Z'_{n,1}$ , the calculation starts from Node  $N - 1$  on the far right first. For the second last Node  $N - 1$ , the ending impedance  $Z_{N-1,1}$  of  $Line(N - 1, 1)$  is equal to the parallel combination of  $Z'_{N,1}$ ,  $Z'_{N,2} \dots$ , and  $Z'_{N,B}$ . For other nodes, the impedance  $Z_{n,1}$  is the terminating impedance viewed from Node  $n$  along the main line (branch number 1). It is equivalent to the *apparent* impedance at Node  $(n + 1)$ ,  $Z_{node-(n+1)}$ . The impedance  $Z_{node-(n+1)}$  is equal to the parallel combination of all transferred impedances of the right adjacent node  $(n + 1)$ ,  $Z'_{(n+1),b}$  for  $b = \{1, \dots, B\}$ . As a result,  $Z_{n,1}$  can be written by

$$Z_{n,1} = \mathbf{P} \left( \vec{Z}'_{n+1} \right) = \frac{1}{\sum_{b=1}^B \frac{1}{Z'_{n+1,b}}} \quad (13)$$

where  $\mathbf{P}(\cdot)$  is the parallelizing operator and the column vector

$$\vec{Z}'_{(n+1)} = \begin{bmatrix} Z'_{(n+1),1} \\ \vdots \\ Z'_{(n+1),B} \end{bmatrix} \quad (14)$$

is the collection of the transferred impedances associated with Node  $(n + 1)$ . Finally, the transfer of the node impedance  $Z_{n,1}$  over the length  $l_{n,1}$  yields the entry  $Z'_{n,1}$  of the matrix  $Z'_{NB}$

$$Z'_{n,1} = \mathbf{T} \left\{ \mathbf{P} \left( \vec{Z}'_{n+1} \right), l_{n,1} \right\} = \mathbf{T} \left\{ Z_{node-(n+1)}, l_{n,1} \right\} \quad (15)$$

As depicted in Fig. 5, the shrinking process is implemented recursively from right to left until  $Z'_{1,1}$  is updated. At this point, the matrix update is complete. Finally, the impedance of desire  $Z_{in} = Z_{node_0} = Z'_{0,1}$  is simply a transfer impedance of  $Z_{node_1}$  over the power line  $Line(0, 1)$  with a length of  $l_{0,1}$

$$Z_{in} = Z'_{0,1} = \mathbf{T} \left\{ \mathbf{P} \left( \vec{Z}'_1 \right), l_{0,1} \right\} \quad (16)$$

The next process is to spread out the source voltage  $V_s$  to the terminating impedance,  $Z_{n,b}$ .

### 3.4. Implementation of Voltage Spreading

The spreading process begins with the initial voltage at Node 0 calculated by

$$V_{node_0} = V_s \left( \frac{Z_{node_0}}{Z_{node_0} + Z_s} \right) \quad (17)$$

The voltage  $V_{n,b}$  on a particular terminating load  $Z_{n,b}$  can be achieved by two following steps. First, the initial voltage  $V_{node_0}$  is forwarded along the main line until it reaches Node  $n$ . There the voltage  $V_{node_n}$  is obtained. Second, the node voltage  $V_{node_n}$  is forwarded along the branch  $b$  for the designated  $V_{n,b}$ .

The computation of  $V_{n,b}$  can be made more systematic by creating a matrix  $\Gamma_{NB}$  of which the entries corresponding to Node  $n$  and Branch  $b$  are given by

$$\Gamma_{n,b} = \frac{Z_{n,b} - Z_{0,n,b}}{Z_{n,b} + Z_{0,n,b}} \quad (18)$$

where  $Z_{0,n,b}$  and  $Z_{n,b}$  are the entries of the characteristic impedance matrix  $Z_{0NB}$  and terminating impedance matrix  $Z_{NB}$ , respectively. The entries of the matrix  $\Gamma_{NB}$  are required to determine the voltages across the power lines. Similarly, the voltages at the terminating load  $V_{n,b}$  can be stored in a resulting matrix  $V_{NB}$  using the same indexing.

Since the voltage  $V_{n,b}$  is a forwarded version of  $V_{node\_n}$  along the branch  $b$ , calculation of  $V_{node\_n}$  is the pathway. The node voltage  $V_{node\_n}$  or  $V_{n-1,1}$  is related to the previous node voltage by

$$V_{node\_n} = V_{(n-1),1} = V_{node\_n(n-1)} \mathbf{F} \{ \Gamma_{n,1}, l_{n,1} \} \quad (19)$$

where  $\mathbf{F}\{\cdot\}$  is the operator that computes the forward voltage gain defined earlier in Eq. (8). Once the  $V_{node\_n}$  is known, the voltage on  $Z_{n,b}$  is given by

$$V_{n,b} = V_{node\_n} \mathbf{F} \{ \Gamma_{n,b}, l_{n,b} \} \quad (20)$$

Combining Eqs. (19) and (20), the voltage  $V_{n,b}$  can be written in a closed form by

$$V_{n,b} = V_{node\_0} \left[ \prod_{m=1}^n \mathbf{F} \{ \Gamma_{m,1}, l_{m,1} \} \right] \mathbf{F} \{ \Gamma_{n,b}, l_{n,b} \} \quad (21)$$

Implementation of the voltage spreading is illustrated in Fig. 6.

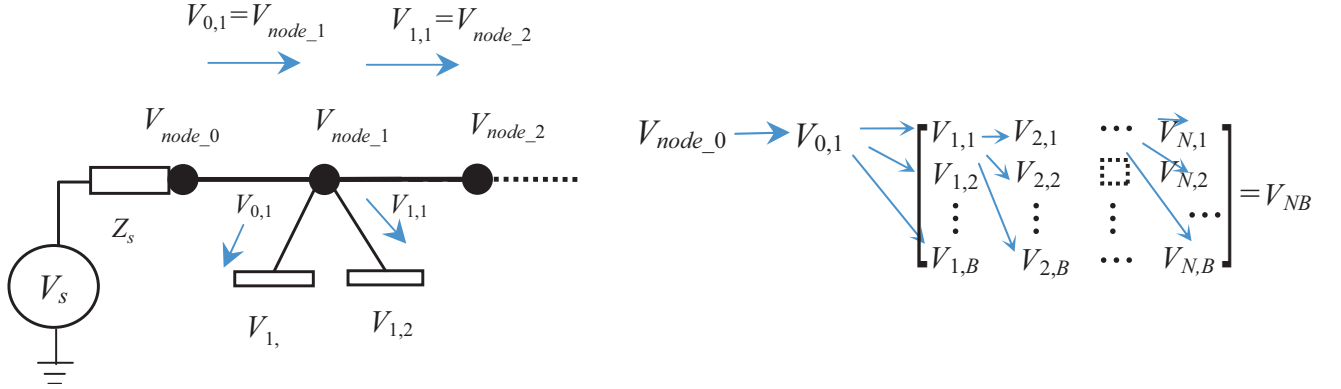


**Figure 6.** Voltage forwarding procedure.

By setting the source voltage flat over the frequency band of interest,  $V_s(f) = 1$ , the transfer function at the terminating load  $Z_{n,b}$  defined by  $H_{n,b}(f) = V_{n,b}(f)/V_s(f)$ , is simply  $V_{n,b}(f)$ . Since  $V_{n,b}(f)$  on any terminating loads can be obtained at the same time, this shrinking-spreading method delivers transfer functions all over the network, simultaneously.

#### 4. RESULTS COMPARISON WITH COMMERCIAL SOFTWARE PACKAGE

In this section, the results from the proposed technique are compared with the results from PSCAD [11], a commercial software package. Since the software package is intended for the power system analysis, the transfer function determination is not handily provided. On the other hand, a rectangular pulse response is a common feature of the software. Therefore, the pulse response will be used as a tool to compare the results obtained from the proposed shrink-spread method and from the commercial software.

The pulse response simulated by the shrink and spread method can be indirectly implemented by the following approach. In time domain, the pulse response  $v_L(t)$  at a destination can be determined by a convolution of the source pulse  $v_s(t)$  and the impulse response from the source to the destination,  $h_L(t)$ . In frequency domain, the Fourier transform of the pulse response  $V_L(f)$  can be achieved by

$$V_L(f) = H_L(f) \cdot V_s(f) \quad (22)$$

where  $H_L(f)$  and  $V_s(f)$  are the Fourier transforms of  $h_L(t)$  and  $v_s(t)$ , respectively. The shrink-spread method determines  $H_L(f)$  while the Fourier transform of a causal rectangular pulse  $v_s(t)$  with an amplitude of  $A$ , a pulse width of  $\tau$  and a delay of  $T_0$  is given by

$$V_s(f) = \tau A \cdot \text{Sinc}(f\tau) \cdot \exp(-j2\pi f \cdot T_0/2) \quad (23)$$

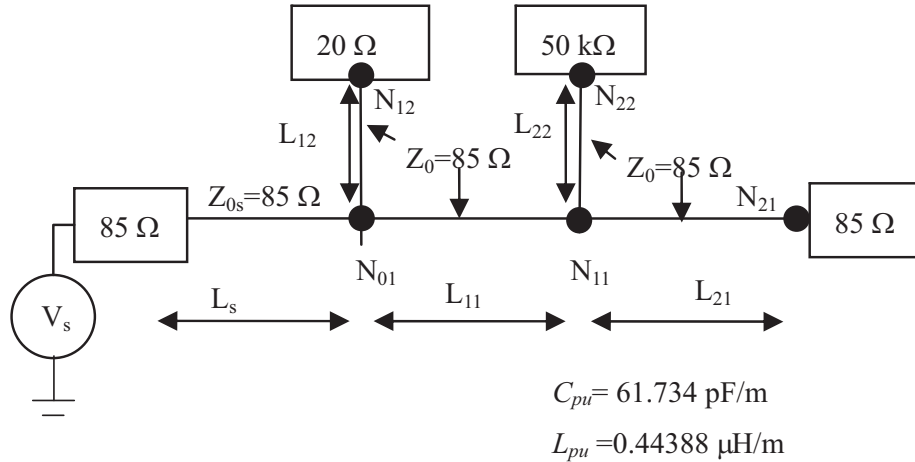


Figure 7. The network to observe the pulse response.

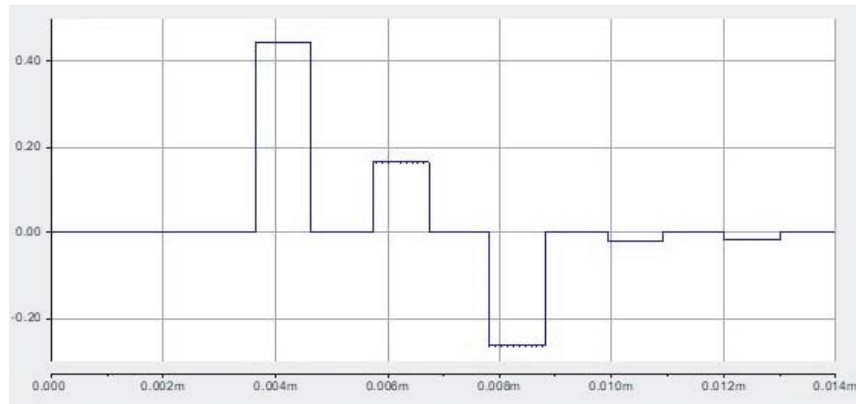


Figure 8. Rectangular pulse response on  $N_{21}$  reported by PSCAD.

Then, the pulse response  $v_L(t)$  is simply the inverse Fourier transform of the product of  $H_L(f)$  and  $V_s(f)$ .

The sample network as shown in Fig. 7 is taken from [12], one of widely cited papers. The source  $V_s$  generates a single rectangular pulse with an amplitude  $A$  of 2 V, a width  $\tau$  of 1  $\mu$ s and a delay of 1  $\mu$ s to drive the network. The resulting waveform observed at  $N_{21}$  by PSCAD is shown in Fig. 8. Meanwhile, the shrink-spread method creates the waveform with a frequency resolution (step) of 1 kHz and the frequency band spans from 0 to 100 MHz, and it is shown in Fig. 9. They are very close to the results by ATP-EMTP, a commercial software reported in [12]. Therefore, the capability to determine the transfer function of the proposed method is confirmed.

### 5. IMPLEMENTATION ON A SAMPLE NETWORK

In this section, the transfer functions throughout a sample home power line network are to be determined by using the proposed shrink-spread method. The merits as communication media at all terminating loads of the branches are measured by using the channel capacity. The topology of the sample network consists of 4 nodes with up to 5 branches connected to them as depicted in Fig. 10.

The cable lengths and the impedances at the ends of the branches are listed in the matrices  $L_{Length}$  and  $Z_{NB}$ , respectively. The terminating impedances on the first row of  $Z_{NB}$  are associated with the equivalent impedances at the interconnections (nodes). They are physically unavailable, so the entries are initially filled with TBD. The characteristic impedances throughout the network are assigned to be 85  $\Omega$ , which is the result of a capacitance of 61.734 pF/m and an inductance of 0.44388  $\mu$ H/m as used

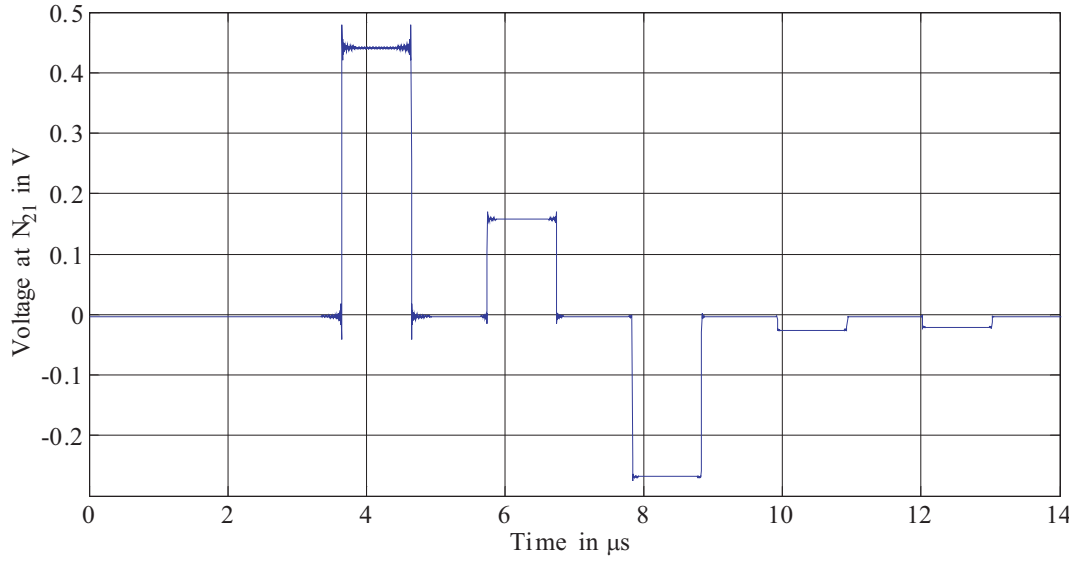


**Figure 9.** Rectangular pulse response on  $N_{21}$  by the proposed shrink-spread method.

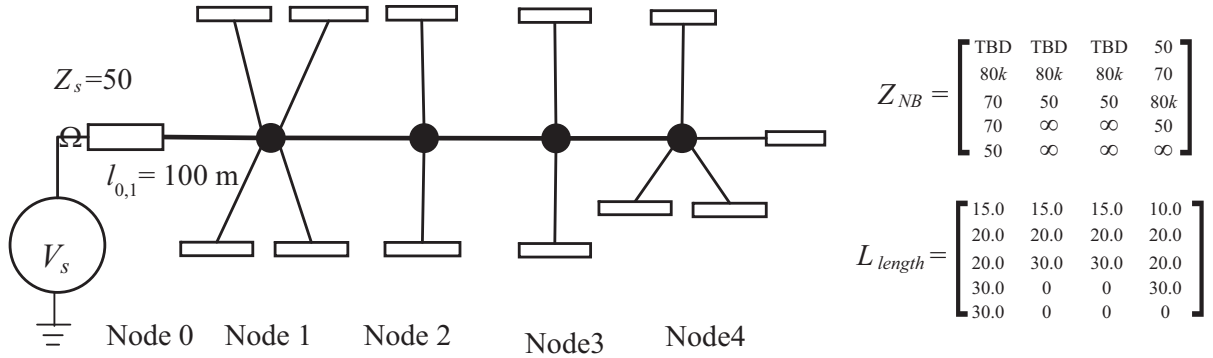


**Figure 10.** Network topology with terminating impedances and the line lengths.

in [12]. The band of interest and the power constraint follow the Homeplug standard, which allows a power spectral density less than  $-50$  dBm/Hz in the 2–30 MHz band [13]. The source impedance  $Z_s$  is assumed to be  $50 \Omega$ .

Signal power spectral densities (PSD) at the terminating impedances are determined from

$$S_{n,b}(f) = |H_{n,b}(f)|^2 \cdot S_{ss}(f) \quad (24)$$

where  $S_{ss}(f)$  is the PSD of the source signal.  $S_{ss}(f)$  is flat at a level of  $-47$  dBm/Hz to ensure that the maximum power density entering the network will not exceed  $-50$  dBm/Hz. With  $-47$  dBm/Hz, power level limit can be reached only when the equivalent impedance of the network  $Z_{in}$  matches to  $50 \Omega$  of  $Z_s$ .

The major types of the noises in typical power line networks are impulsive and background noise. However, in this simulation, only the color background noise present at the load  $Z_{n,b}$  is to be considered. Although the impulsive noise dominates the channel performance, it is not taken into account. The background noise PSD as given in [14] is described by

$$N_{PSD}(f) = a + b \cdot f^c \text{ dBm/Hz} \quad (25)$$

where  $f$  is the frequency in MHz. The noise PSD is monotonously decreasing, and the asymptotic noise floor in the higher frequency band is  $a$  dBm/Hz. The values of  $a$ ,  $b$  and  $c$  as given in the literature for the worst case are  $-145$ ,  $53.23$  and  $-0.337$ , respectively.

Channel capacity is commonly used as a measure to evaluate the link merit. The discrete frequency version of the channel capacity calculation at the terminating impedance  $Z_{n,b}$  is given by [15]

$$C_{n,b} = \Delta f \sum_{m=M_1}^{M_2} \left[ \log_2 \left( 1 + \frac{S(m\Delta f) |H_{n,b}(m\Delta f)|^2}{N(m\Delta f)} \right) \right] \quad (26)$$

In this simulation, the calculation of  $C_{n,b}$  covers a band ranging from  $M_1 \cdot \Delta f = 2$  MHz to  $M_2 \cdot \Delta f = 30$  MHz.

The signal power spectral densities at the selected loads  $Z_{1,5}$ ,  $Z_{2,3}$ ,  $Z_{3,3}$  and  $Z_{4,1}$  are shown in Fig. 11, and the effective channel capacities in Mbps at all loads are summarized in the matrix  $C_{NB}$ .

$$C_{NB} = \begin{bmatrix} 554 & 490 & 397 & \mathbf{375} \\ 722 & 655 & 601 & 382 \\ 596 & \mathbf{515} & \mathbf{451} & 508 \\ 597 & - & - & 358 \\ \mathbf{572} & - & - & - \end{bmatrix} \quad (27)$$

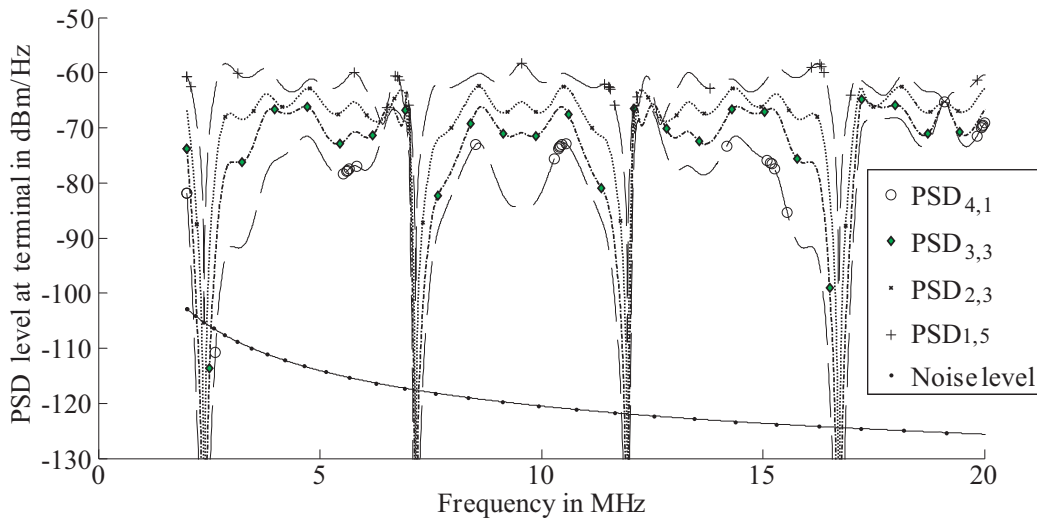


**Figure 11.** PSD of the signals at the selected loads and PSD of the background noise.

Note that  $C_{n,1}$  for  $n = 1$  to 3 on the first row of  $C_{NB}$  do not physically exist. They are available in the matrix because the equivalent transfer functions at the nodes exist. The calculation of the channel capacities is then possible.

## 6. SUMMARY AND CONCLUSION

In this paper, a recently-proposed alternative method to determine the transfer functions on the power line network is reviewed, analyzed and further developed. The method shrinks the entire network into a single impedance then spreads out the voltage to all destination loads. Its major advantages over the existing technique are simplicity and intuitiveness with an essential feature on the capability to monitor the transfer functions throughout the network. The development delivers a recursive form for the shrinking process and a production form for the spreading processes. Furthermore, this paper describes the network in a matrix form which makes implementation of the method computation-friendly. Lastly, a demonstration of using this method on a sample network is provided. The capability of this method is thus confirmed. This method, therefore, is an alternative to evaluate the transfer functions with noticeable advantages.

It is assumed that there are no sub-branches in the network topology. To deal with the case, the proposed method needs some modification. The sub-branches, in fact, can be shrunk into one impedance

by the same shrinking process. Then, the proposed method can be applied. This method does discard all features other than the impedances and voltages. Those might be needed in some scenarios. Finally, the major drawback of this method is that it still needs to evaluate the transfer function one frequency at a time. The future research possible aims to reduce this burden.

## REFERENCES

1. Zimmermann, M. and K. Dostert, "A multi-path signal propagation model for the power line channel in the high frequency range," *Proc. 3rd Power-Line Communications and Its Applications*, 45–51, 1999.
2. Anatory, J., M. M. Kissaka, and N. H.Mvungi, "Channel model for broadband power line communication," *IEEE Transactions on Power Delivery*, Vol. 22, No. 1, 135–141, Jan. 2007,
3. Anatory, J., N. Theethayi, and R. Thottappillil, "Power-line communication channel model for interconnected networks — Part I: Two-conductor system," *IEEE Transaction on Power Delivery*, Vol. 24, No. 1, 118–123, Jan. 2009.
4. Galli, S. and T. Banwell, "A novel approach to the modelling of the Indoor power line channel — Part II: Transfer function and its properties," *IEEE Transaction on Power Delivery*, Vol. 20, No. 3, Jul. 2005.
5. Ravelo, B. and O. Maurice, "Kron-branin modeling of Y-Y-tree interconnects for the PCB signal integrity analysis," *IEEE Transactions on Electromagnetic Compatibility*, Vol. 59, No. 2, Apr. 2017, 411–419.
6. Ravelo, B., "Theory on asymmetrical coupled-parallel-line transmission and reflection zeros," *Int. J. Circ. Theor. Appl.*, Vol. 45, No. 11, 1534–1551, Nov. 2017.
7. Ravelo, B., "Behavioral model of symmetrical multi-level T-tree interconnects," *Progress In Electromagnetics Research B*, Vol 41, 23–50, 2012.
8. Berger, L. T. and G. Moreno-Rodríguez, "Power line communication channel modelling through concatenated IIR-filter elements," *Journal of Communications*, Vol. 4, No. 1, 41–51, Jan. 2009.
9. Li, B., D. Mansson, and G. Yang, "An efficient method for solving frequency responses of power-line networks," *Progress In Electromagnetics Research B*, Vol. 62, 303–317, 2015.
10. Khongdeach, T. and W. Chongburee, "A method to analyze communication bandwidth and pulse response of power lines with branches using backward impedance transform technique," *Proc. of the 10th ECTI-CON*, 1–5, 2013.
11. Manitoba HVDC Research Centre [Online], Available: <https://hvdc.ca/pscad/freeversion>, Accessed on: May 1, 2018.
12. Anatory, J. and N. Theethayi, "Comparison of different channel modeling techniques used in the BPLC systems," *World Academy of Science, Engineering and Technology International Journal of Electrical and Computer Engineering*, Vol. 5, No. 8, 1034–1040, 2011.
13. Yonge, L., et al., "An overview of the HomePlug AV2 technology," *Journal of Electrical and Computer Engineering*, Vol. 2013, Article ID 892628, 20 pages, 2012, Internet: <https://www.hindawi.com/journals/jece/2013/892628/>, Mar. 10, 2018.
14. Esmailian, T., P. G. Gulak, and F. R. Kschischang, "A discrete multitone power line communications system," *Proc. ICASSP*, Vol. 5, 2953–2956, 2000.
15. Lazaropoulos, A. T., "New coupling schemes for distribution broadband over power line (BPL) networks," *Progress In Electromagnetics Research B*, Vol. 71, 39–54, 2016.